

5. PETROGRAPHY AND GEOCHEMISTRY OF GRADED VOLCANICLASTIC SEDIMENTS AND THEIR CLASTS, LEG 129¹

G. J. Lees,² G. Rowbotham,² and P. A. Floyd²

ABSTRACT

Samples collected from the coarse basal portions of mid-Cretaceous volcaniclastic turbidites from the Mariana and Pigafetta basins are remarkably similar in terms of the petrographic and chemical features of their igneous clasts and bulk rock composition. Clasts of magmatic origin are dominated by glassy vesicular shards, variably phyrlic, holocrystalline basalts, and crystal fragments (olivine, clinopyroxene, plagioclase, amphibole, and biotite). The composition of the pyroxenes and amphiboles are typical of those found in differentiated hydrous alkali basalts. The bulk chemical composition of the volcaniclastites (based on stable incompatible elements and their ratios in highly vitric samples) is characteristic of alkali basalts found in within-plate oceanic eruptive environments. Miocene volcaniclastites from Site 802 are broadly similar to the Cretaceous samples in terms of clast type and bulk composition, and have also been derived from an oceanic alkali basalt source. The chemistry of the Miocene volcaniclastites differ, however, in having distinctive Zr/Y and Zr/Nb ratios and a more restricted chemical composition. The magmatic products of nearly emergent seamounts within the western Pacific basins appears to have been dominated by alkali basalt volcanism during the mid-Cretaceous and also the Miocene.

The highly vitric nature of the Cretaceous and Miocene volcaniclastites, together with the morphology and vesicularity of their shards, suggests that they are the reworked (via mass flow) products of hyaloclastite accumulations produced in a shallow-water eruptive environment, such as that adjacent to nearly emergent seamounts or ocean islands. The association of ooids, reefal debris, and, in rare cases, woody material with the volcaniclastites supports their shallow-water derivation.

INTRODUCTION

Basins within the central and western Pacific Ocean often contain large volumes of volcaniclastic material that represent the products of reworked, turbidite current-deposited, hyaloclastites derived from adjacent seamounts and ocean islands (Winterer, 1973; Rea and Vallier, 1983). Many of these volcanogenic sediments are representative of the "mid-Cretaceous" volcanic event (Schlanger et al., 1981; Schlanger and Moberly, 1986; Larson and Schlanger, 1981) that roughly covered the period from the Aptian to the Campanian. During this time extensive regional volcanism built both edifice structures, oceanic plateaus (for example, Ontong-Java), and submarine extrusive complexes, such as Nauru Basin (Larson and Schlanger, 1981) and possibly the sequence at Site 802 (Floyd et al., this volume).

Volcaniclastic sediments of broadly middle Cretaceous age were also recovered from Sites 800 and 801 in the Pigafetta Basin and Site 802 in the Mariana Basin (Fig. 1) during Leg 129 (Lancelot, Larson, et al., 1990). In addition, about 200 m of volcanogenic turbidites of Miocene age were recovered from the upper part of the Site 802 succession. Although the Miocene volcaniclastics are situated in a relatively isolated portion of the Mariana Basin, well away from readily identifiable seamounts and ocean islands, seismic profiles suggest that the sequence thickens towards the south and indicates a possible source in the Caroline Islands (Lancelot, Larson, et al., 1990).

In this paper we identify the characteristic petrographic and chemical features of both Miocene and Cretaceous volcaniclastites, and their individual clasts, to determine the composition and nature of edifice-building volcanism in the western Pacific. Apart from the relatively few subaerial structures in this vast region, the abundant volcanogenic sediments provide a record of the volcanic history and magmatic character of the eruptions. These features are significant in the broader context of the "synchronous" mid-Cretaceous volcanic

event and its association with a widespread lithospheric thermal anomaly (Haggerty et al., 1982; Larson, 1991).

ANALYTICAL METHODS

Samples of volcaniclastic material (75) were selected from the coarser basal sections of turbidites from Sites 800, 801, and 802 for detailed petrographic and geochemical study. Of these, 19 were from the Miocene units in Hole 802A and 56 from the Cretaceous units at all three sites. Thin sections were made of virtually all samples. From these, six representative samples (from Units IIA and V of Site 802; Unit IV of Site 801; Unit IV of Site 800) were selected for the chemical analysis of their constituent phases, using either a Cameca (Camebax) or Cambridge Instruments Geoscan electron microprobe fitted with a Link System energy-dispersive spectrometer. The operating conditions were 15 kV and 3.5×10^{-8} Å and a spot size of about 3 µm, except for the analysis of hydrous phases when the beam was defocused. The calibration was determined against metal, oxide, and silicate standards. An estimate of the accuracy and precision of this technique is reported in Dunham and Wilkinson (1978). Seventy-three samples were analyzed for major and trace elements by wavelength-dispersive X-ray fluorescence techniques using an ARL 8420 fully automated sequential spectrometer (for further details, see Floyd and Castillo, this volume). X-ray diffraction techniques were used to identify the clay mineral and zeolite species, using a Phillips PW1700 fully automated diffractometer. Before diffraction, samples were centrifuged (to separate the <2 µm size fraction) and sedimented onto a glass mount, and then subsequently glycolated and heat treated before rediffraction.

VOLCANIC SEDIMENTS IN OCEAN BASINS

The occurrence of volcaniclastic rocks in sediments of the deep oceans has frequently been recorded in cores obtained by deep-sea drilling (for example, Bowles et al., 1973; Schmincke et al., 1978; Scheidegger et al., 1978; Houghton, 1979; Kelts and Arthur, 1981; Schmincke, 1981, 1983a, 1983b; Rea and Vallier, 1983; Floyd, 1986a, 1986b; Viereck et al., 1986). In the western Pacific Ocean, especially

¹ Larson, R. L., Lancelot, Y., et al., 1992. *Proc. ODP, Sci. Results*, 129: College Station, TX (Ocean Drilling Program).

² Department of Geology, University of Keele, Staffordshire, ST5 5BG, United Kingdom.

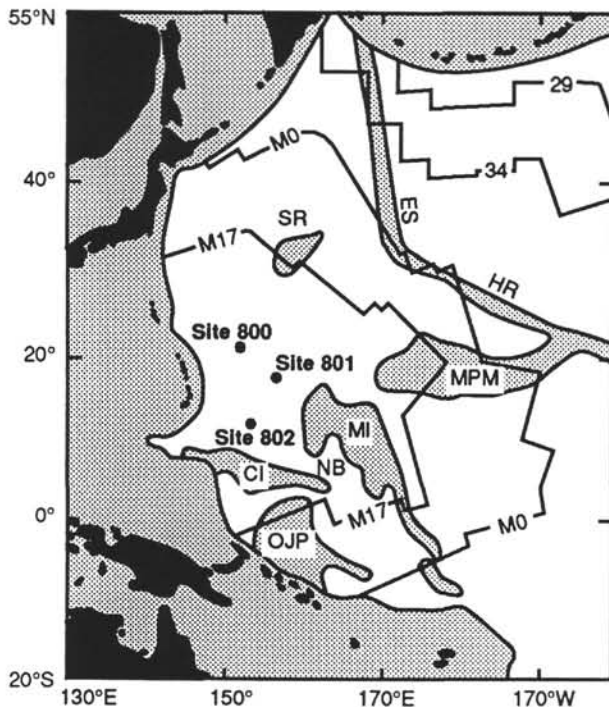


Figure 1. Map of the western Pacific Ocean, showing the position of Leg 129 Sites 800, 801, and 802 (Lancelot, Larson, et al., 1990). Feature abbreviations are as follows: Caroline Islands (CI), Ontong Java Plateau (OJP), Marshall Islands (MI), Nauru Basin (NB), Mid-Pacific Mountains (MPM), Shatsky Rise (SR), Hawaiian Ridge (HR), and Emperor Seamounts (ES). Jagged contours represent magnetic lineations and unshaded areas represent normal Pacific oceanic crust. Shaded areas represent volcanic edifices with thickened crustal sections, as well as younger areas beyond the Pacific subduction zones.

adjacent to seamounts, they form thick turbidite and debris flows within the pelagic sedimentary pile and represent a significant proportion of the sediment fill to local deep basins.

The volcanoclastic sediments encountered during Leg 129 are remarkably uniform in their character and composition, varying in grain size between coarse pebbly sandstone and claystone. The maximum size fractions in the graded sediments of both Miocene and Cretaceous age are dominated by mostly medium to coarse vitric tuffs, with lithic tuffs as a minor component. Fine-grained, bedded tuffaceous sediments also occur as fragments or lapilli (Fisher and Schmincke, 1984) within the lithic-rich units. The primary igneous clast sizes very rarely exceed the modal grain size for the host rock. The coarse basal portions of these graded volcanoclastic sequences were sampled throughout both the Miocene of Site 802 and the Cretaceous encountered in all three sites (Fig. 2). A combination of bulk-rock chemistry, electron microprobe analysis, and petrographic examination has been employed to identify the magmatic character of the volcanogenic component of the sediments.

PETROGRAPHY OF PRIMARY COMPONENTS

The marked similarities that exist in the nature of the volcanoclastites from all three sites allow their detailed petrographic characteristics to be described together. There are two main aspects to the petrography of the deep-sea volcanoclastic deposits: (1) the nature of the primary components and their variation throughout the sequence, and (2) the nature of their alteration. The first will be considered below, and the second in the next section. A summary and comparison of major characteristics is given in Table 1 (on microfiche in the back of this volume) and various petrographic features are illustrated in Plate 1.

The primary components of these deposits may be divided into five groups: (1) lithic components—mainly basaltic clasts, with some tuffaceous lapilli, (2) fragmented crystals, (3) vitric components—shards and scoriae, (4) nonvolcanogenic components, such as biogenic fragments and carbonate debris, and (5) fine-grained interstitial material ("matrix").

Lithic Clasts

Volcanogenic lithic clasts are essentially of two types, with very different origins. Fine-grained glassy and crystalline basaltic clasts represent the spalled off rinds of lava flows, whereas lithified tuffaceous clasts were probably incorporated into the density currents as rip-ups from the seafloor.

Basaltic Clasts

Basaltic clasts of various types are ubiquitous throughout both the Cretaceous and Miocene sequences, though in the vitric-rich horizons they may make up less than 1% of the clastic component. The igneous lithic clasts are usually angular to subangular in shape and almost never have a grain size which is larger than the modal value for the deposit as a whole. The following types have been observed: (1) fine-grained porphyritic basalt with large phenocrysts of olivine, (2) holocrystalline (occasionally clinopyroxene phyrical) basalt with an interlocking matrix of long prismatic plagioclase and interstitial clinopyroxene and ore phases, (3) plagioclase-rich holocrystalline rock with a trachytic texture, insufficiently mafic to be called basalt, (4) variolitic-textured basalts with prominent skeletal microphenocrysts of clinopyroxene, often in glomerophytic groups with plagioclase, (5) very fine-grained, dark, hypocrySTALLINE basalt with microlites of clinopyroxene and plagioclase, and sometimes pyroxene microphenocrysts, and (6) tachylite with plagioclase microlites, often vesicular, with rare olivine megaphenocrysts.

All the crystalline phases in the basaltic clasts are unaltered in the Miocene sequence, whereas partial or complete alteration to clays (\pm zeolites) is a common feature in the Cretaceous successions of Sites 800 and 802. However, even here completely altered clasts often coexist in intimate juxtaposition with completely fresh ones. Site 801 clasts are invariably all altered. Of the various clast types the fine-grained tachylite and hypocrySTALLINE basalt fragments are much more common than the others, with shapes often dictated by the outer walls of vesicles. Since these clasts probably originated as comminuted pillow lava rinds, the dominance of this clast type is perhaps not surprising. Holocrystalline fragments, representing the internal portions of lava flows, are much less frequent. The occurrence of tachylite clasts and sideromelane shards, both containing fresh olivine phenocrysts, in the Miocene of Site 802 (Unit IIA) suggests that both materials were being derived via fragmentation from the same petrographic unit or eruptive event.

Lithified Tuffaceous Claystones and Siltstones

Virtually all the clasts which are of larger size than the modal grain size of the host rock matrix are composed of poorly laminated, sub-rounded to subangular, tuffaceous claystones or siltstones (for example, upper units of Site 802). They are usually slightly elongated and often blocky, with an aspect ratio varying between 6:1 and 1:1 and a length up to 11 mm. Lamination is not always parallel to the long axis of the clasts except where the aspect ratio approaches 5:1 or more. They are commonly composed of a fine clay mosaic, but occasionally larger crystal fragments, usually plagioclase, and rare nanofossils have been observed. Sometimes these clasts may have dark brownish (oxidized) rims. Their laminated, fine-grained texture indicates that they were deposited from the water column as tuffaceous (subaerial?) debris onto the seafloor. This was subsequently eroded by the scouring action of

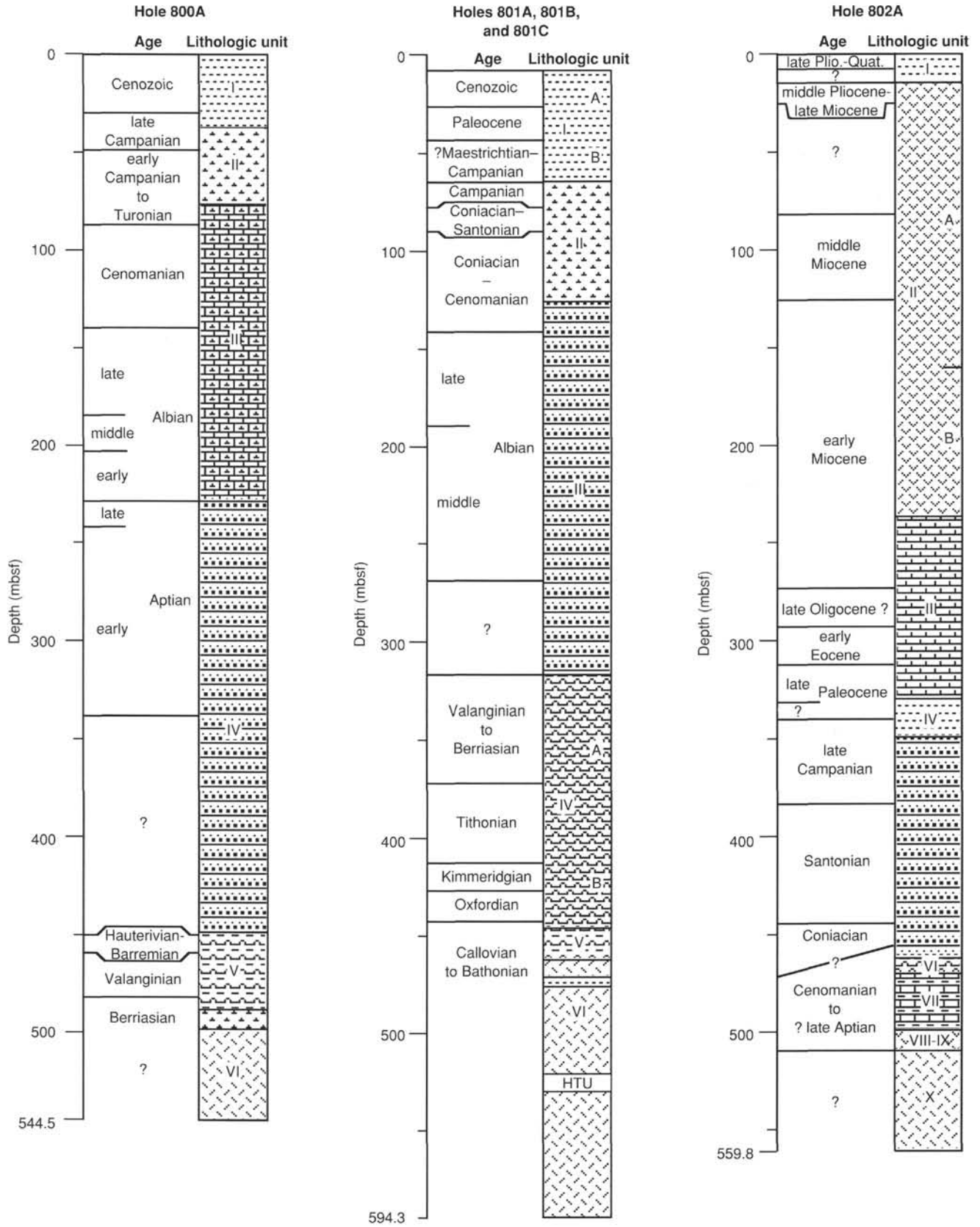


Figure 2. Stratigraphic depth correlation diagram for Sites 800, 801, and 802 (Lancelot, Larson, et al., 1990), showing location of Cretaceous (small and large block ornament) and Miocene (dotted V ornament) volcaniclastite units.

density currents carrying predominantly hyaloclastite materials, with which they became subsequently mixed.

Crystal Fragments

The fragmented crystal phases present in the volcanoclastites are the same as the phenocrysts observed within the vitric shards and lithic clasts. Observations recorded in this section thus refers to both fragments and phenocrysts.

Olivines

Olivine crystals are common in both the Miocene and Cretaceous volcanoclastites. In the basal portion of the Miocene unit IIA (Site 802), it forms the dominant crystal phase, both as fragments and phenocrysts. Here, olivine may be present as subhedral to anhedral fragments up to 3 mm long, or occasionally form euhedral crystals embedded in fresh glass (for example, Samples 129-802A-15R-1, 19–24 cm, 129-802A-15R-1, 128–133 cm, and 129-802A-16R-1, 119–123 cm). Overall they range in composition from Fe_{77-85} (Fig. 3), although zoning is minimal. In the Cretaceous volcanoclastites olivines are very rarely preserved in the fresh state, being invariably pseudomorphed by pale green smectite.

Spinel

Spinel is found as opaque euhedral octahedra in the olivine crystals of some Miocene volcanoclastites (for example, Samples 129-802A-14R-2, 81–85 cm, 129-802A-15R-1, 128–131 cm, and 129-802A-16R-1, 119–123 cm). The Cr_2O_3 and TiO_2 contents are high (up to 46% and 5%, respectively) and indicate they are typical chromian spinels. The $Cr/(Cr + Al)$ ratio increases with increased $Mg/(Mg + Fe^{2+})$, whereas there is a negative correlation of Ti against $Mg/(Mg + Fe^{2+})$. This probably reflects the proportion of the Fe-Ti oxide end-member in the spinel (Fig. 4).

Pyroxenes

Clinopyroxene occurs both in lithic clasts and as discrete crystals in a fine-grained smectite groundmass. They are by far the most ubiquitous fragmental crystal species, although in the olivine-rich horizons near the base of Unit IIA at Site 802, they are uncommon. Throughout most of the volcanoclastic sequences they are the only fresh primary crystal phase preserved.

In the Cretaceous volcanoclastites, pyroxenes largely occur as discrete fractured crystals with diopside and ferrosalite compositions (for example, in Samples 129-800A-33R-4, 146–150 cm, and 129-800A-31R-2, 45–50 cm). These compositions are indicative of differentiated alkali basalt suites (Wilkinson, 1956). There are differences between the two samples in that pyroxenes in the former sample contain less Ti, Al, and Fe (and exhibit a limited compositional range from $Ca_{48}Mg_{44}Fe_8$ to $Ca_{45}Mg_{48}Fe_7$) than those in the latter (with a very wide range from $Ca_{51.5}Mg_{4}Fe_{12}$ to $Ca_{47.6}Mg_{9}Fe_{44}$) (Fig. 5). Despite this variation between crystal fragments, there is only a restricted range of intracrystalline variation. Pyroxenes in the Miocene volcanoclastites are diopside to calcic augite in composition, again typical of alkaline basaltic rocks.

Amphiboles

Amphiboles occur within a particular zone of the Site 800 lower Aptian sequence between Cores 30R and 32R (Unit IV) They are discrete crystals (?phenocrysts) and have not been found enclosed within lithic clasts. The dark brown pleochroic amphiboles in Sample 129-800A-31R-2, 45–50 cm, were analyzed and are titaniferous ferroan pargasites (Leake, 1978) with $Mg/(Mg + Fe^{2+})$ values between 0.47 and 0.71. Amphiboles of this composition are typical of fractionated, hydrous, alkali basaltic rocks (Henderson and Gibb, 1988).

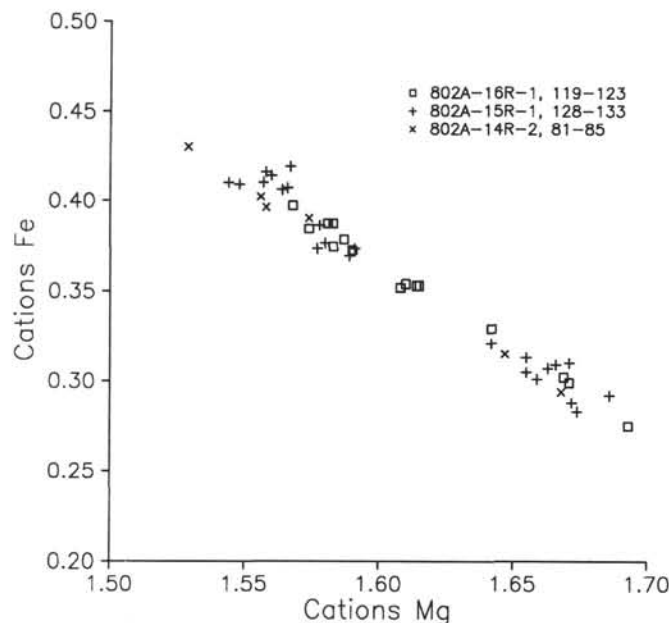


Figure 3. Compositional variation in fresh olivines from Miocene volcanoclastites (Hole 802A).

Micas

Primary mica is extremely rare in these sediments and then only found in association with pargasitic amphibole. Small irregular flakes of red brown biotite have been identified as crystal debris in only two samples from the upper portion of Unit IV at Site 800.

Feldspars

Plagioclase is a ubiquitous phase, though its presence as a significant component of the crystal debris is patchy, being largely concentrated in specific parts of the Cretaceous volcanoclastites at Sites 802 and 800. In Sample 129-800A-31R-2, 125–130 cm, fresh plagioclase occurs both as discrete crystal fragments (An_{64-66}) and in lithic clasts (An_{64-77}) with compositions typical of moderately evolved basaltic rocks. In an analyzed Miocene example (Sample 129-802A-14R-2, 81–85 cm) the plagioclase feldspars had a similar composition varying from An_{65} to An_{69} .

Vitric Material

Vitric material is by far the dominant volcanogenic component in nearly all the volcanoclastite units sampled. In some cases, devitrification and alteration have rendered it very difficult to identify as such, particularly in the fine-grained matrix that supports the clasts. Much of this matrix is now largely composed of a mosaic of clay minerals, some of which probably replaced an original fine glassy ash.

The shard classification used by Schmincke and coworkers has been confirmed and used in this study (Schmincke et al., 1982; Fisher and Schmincke, 1984; Viereck et al., 1986). The same range of shard types was encountered in both Miocene and Cretaceous deposits. Simple shards of both spalling and bubble wall types are the most common, particularly in the units considered to be redeposited hyaloclastites. Compound shards of both blocky and, more spectacularly in the coarse grained volcanoclastites, scoria type, also occur in significant proportions. The highly intricate and delicate cusped shapes of large shards controlled by vesicle margins are commonly preserved, while large multichambered vesicular scoriae are common in both the Miocene and the Cretaceous volcanoclastites of Sites

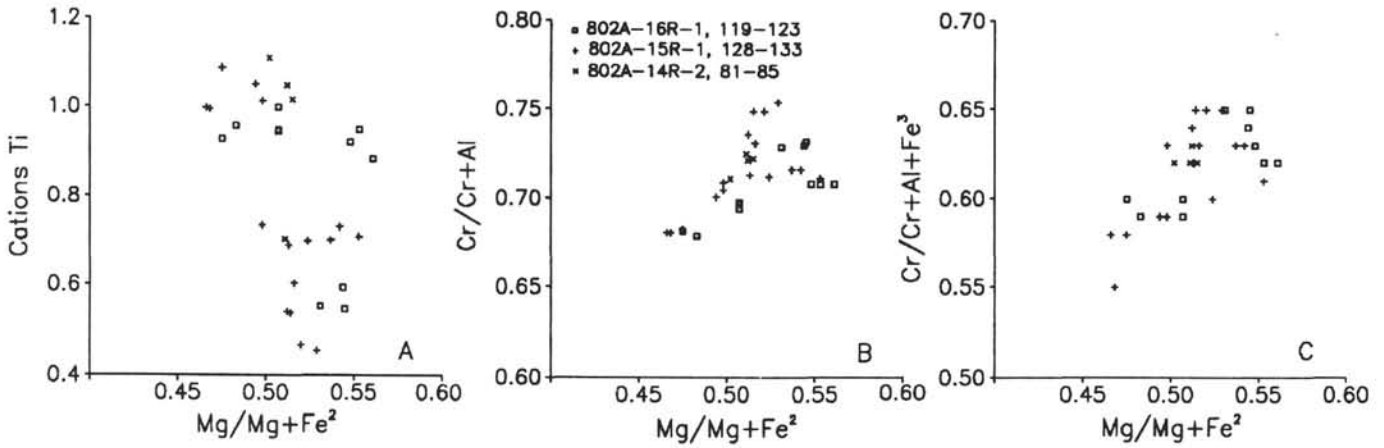


Figure 4. Compositional variation in spinels enclosed in olivine from Miocene volcanoclastites (Hole 802A).

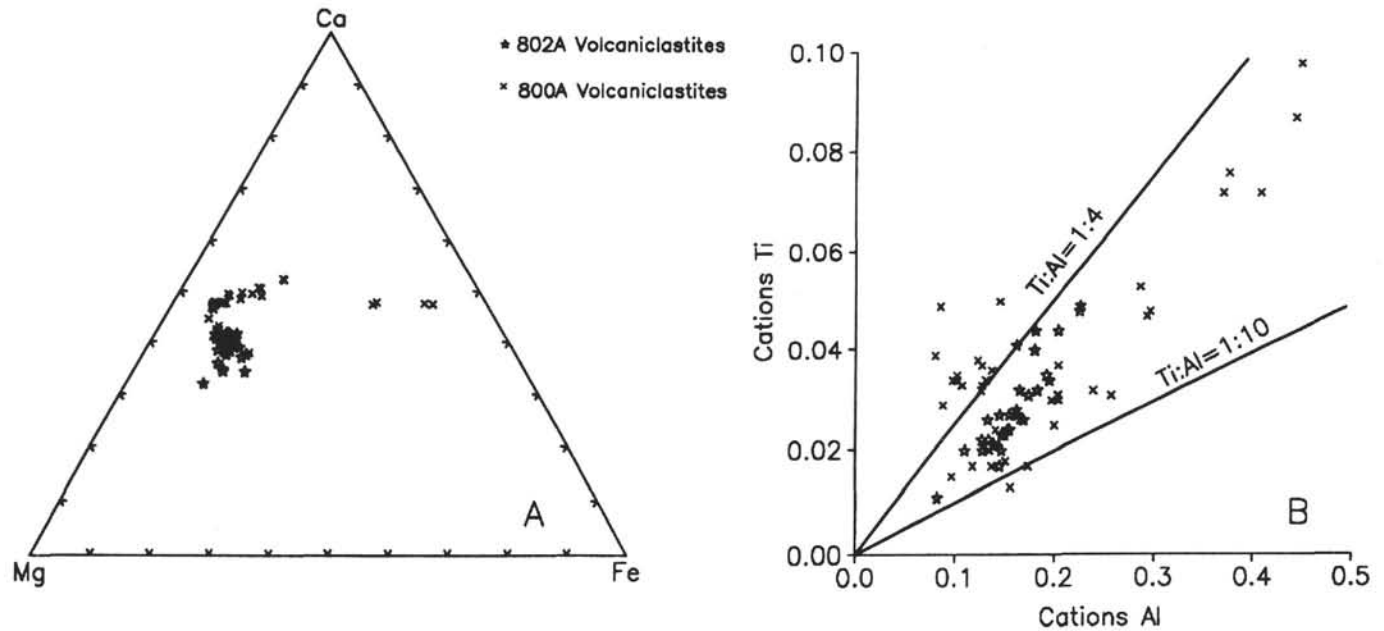


Figure 5. Compositional variation of clinopyroxene crystal fragments in Cretaceous (Hole 800A) and Miocene (Hole 802A) volcanoclastites. The greater range of compositions (from diopside to ferrosalite) for the Cretaceous clinopyroxenes suggests they have been derived from a wider range of fractionated parental basalts than the augites of the Miocene samples.

800 and 801. Vesicles are invariably infilled with radiating fibrous smectites, as described previously from other sites (for example, Viereck et al., 1982, 1986; Floyd, 1986a), although zeolites and sometimes calcite (especially at Site 801) has been noted.

ALTERATION

Chemistry of Secondary Phyllosilicates

Celadonites and an array of smectite compositions occur in the volcanoclastics. Adamson (1981) devised a recalculation method to reveal the variation in di- and tri-octahedral smectites in oceanic basalts (see Rowbotham and Floyd, this volume, for details) whereby the cations in the tetrahedral and octahedral sites should total 12 for dioctahedral smectites, 14 for trioctahedral smectites, and 15.71 for prochlorite. Values for the Leg 129 phyllosilicates indicates that they are predominantly trioctahedral smectites rather than chlorites or smectite-chlorite mixed layer minerals.

The formula for smectites can be generalized as: $(Ex^+)_c (Al, Fe^{3+})_m (Mg, Fe^{2+})_{(4+2t-m)} Si_{8-5} Al_5 O_{20} (OH)_4$, where Ex^+ represents

interlayer cations, Ca, Na, and K. All the analyses of smectitic clay minerals from the Cretaceous and Miocene volcanoclastics contain Ca^{2+} , Na^+ , and K^+ as interlayer cations, their total value of which increases from <0.2 (replacing olivine) to about 0.8 in the majority of other replacement situations. This interlayer charge confirms that the phyllosilicates are chemically smectites rather than chlorites. Figure 6 shows the variation between lattice and interlayer cations in phyllosilicate samples selected from Sites 800 and 802. Relative to the smectites, which have highly variable interlayer cation contents and Fe/Mg ratios, the celadonites from Hole 800A are characteristically high in K and more restricted in their range of chemical composition. The variable Fe/Mg ratios shown by smectites from the Miocene volcanoclastites is a reflection of differential host replacement, especially primary minerals versus fine-grained matrix.

One example from the Cretaceous (Sample 129-800A-33R-4, 146–150 cm) was selected for detailed analysis because of the range of different sites of alteration shown by the smectites in plagioclase, olivine pseudomorphs, zoned vesicles, and matrix, with various colored clay minerals (Table 2 on microfiche in the back of this volume). The

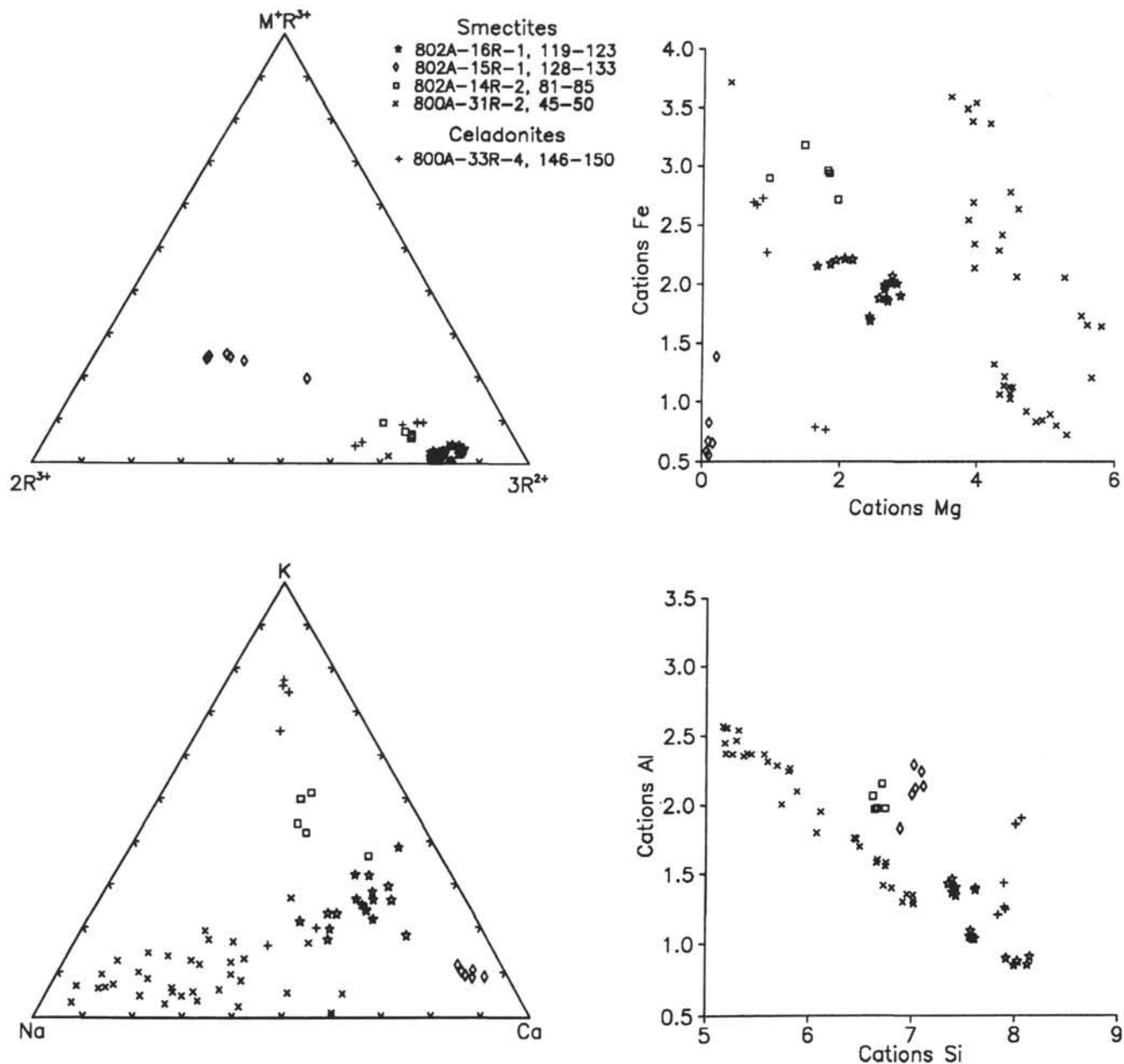


Figure 6. Compositional variation in phyllosilicates (largely smectites, some celadonites) from Cretaceous (Hole 800A) and Miocene (Hole 802A) volcanoclastites. Triangular M^+R^{3+} - $3R^{2+}$ - $2R^{3+}$ diagram modified after Velde (1985).

range of mineral replacement is similar to that described by Viereck et al. (1986), but in the present study the sites of alteration were analyzed separately. The data indicate a variety of compositions which appear to be site specific. The olivine pseudomorphs are the most magnesian with the lowest Ex^+ values indicating that they are close to the talc-pyrophyllite boundary with the saponites (Adamson, 1981). The green replacement phase of plagioclase, however, is more Fe-rich, but still aluminous, that is, an Al-saponite. The smectites in vesicles have quite distinct compositions with those in the rims having high Fe/Mg ratios and intermediate Ex^+ contents, whereas those in the cores show the opposite and an Ex^+ component of mainly sodium (Table 2 on microfiche).

Alteration of Glass Shards

Although fresh glass (sideromelane) is preserved in the Miocene of Site 802 (towards the base of Unit IIA), vitric material has mostly

undergone alteration either wholly or partially to clays. Studies of the alteration of basaltic glass in pillow lavas under low temperature conditions abound, but less so for hyaloclastites (for example, Floyd and Rowbotham, 1986; Schmincke, 1983a; Viereck et al., 1982, 1986).

Glass shards from the Miocene volcanoclastics (Site 802, Unit IIA) provide excellent examples of the glass to palagonite to smectite alteration transition. In Samples 129-802A-15R-1, 19–24 cm, 129-802A-15R-1, 128–133 cm, and 129-802A-16R-1, 119–123 cm, the yellow-brown fresh glass is surrounded by dark brown isotropic palagonite and finally a zone of brown smectite. Mechanisms detailing the formation and the concomitant chemical changes during the palagonitization process have been reviewed by Zhou and Fyfe (1989). Using altered glass samples from Deep Sea Drilling Project (DSDP) Site 335, they show that there is a coupled increase in both Fe and Ti from the fresh basalt glass to the palagonite. In the present study Ti increases from glass to palagonite, but then decreases sharply in the authigenic smectite, whereas Fe decreases from the glass to

palagonite and then increases sharply to a maximum in the clay. MgO follows the same pattern as FeO. The MgO/(MgO + FeO) ratio is about 0.35–0.45 in the glass, drops to about 0.11 in palagonite and rises again to a similar value in the smectite (0.27–0.39). The accumulation of Fe and Ti in palagonite was used as a maturity index by Staudigel and Hart (1983), but the different behavior of Fe from study to study inhibits its widespread application as a measure of glass aging. The alkali metals and alkali earth elements provide a contrast in behavior in these samples. The CaO content maintains its concentration from the glass to the palagonite in all three samples (10–11 wt%), but drops markedly in the smectitic clay. Na₂O behaves in a different manner to CaO; the concentration decreasing from glass (2.50–3.50 wt%) to essentially similar concentrations in the palagonite and the smectite (0.5–0.9 wt%). Zhou and Fyfe (1989) show that CaO decreases markedly in their sample from glass to palagonite, but Na₂O behaves in an analogous way to that in our samples. K₂O is progressively enriched from the glass (0.60–0.90 wt%) through palagonite (1.00–2.00 wt%) to smectite (up to a maximum of 4.00 wt%). Such an increase in K in glass to smectite alteration is well documented (Honnorez, 1981) and represents the uptake of K⁺ from seawater, leading to K-rich smectites.

Bulk X-ray Powder Diffraction Analysis

The <2- μ m fraction of 58 Cretaceous and 19 Miocene volcanoclastic samples were analyzed by X-ray powder diffraction. The overall X-ray patterns are typical of altered oceanic basalts and basic volcanoclastites and confirm the presence of clay minerals, zeolites, silica polymorphs, and calcite (Table 3 on microfiche in the back of this volume).

The clay fraction shows the presence of a clay mineral with a broad asymmetric peak in the 12–15- \AA region, and an 10- \AA peak indicative of celadonite (Table 3 on microfiche). All the samples were treated with ethylene glycol and the d(001) smectite shifted to higher “d” spacings, while the celadonite peak remained undisturbed. The second effect of glycolation was to increase the peak height/width ratio and the symmetry of d(001) smectite. On heating the samples to 550°C for 1 hr, the d(001) smectite collapsed to 9.6–10 \AA in all samples. The shift to higher “d” spacings and collapse to about 10 \AA indicates that the main clay minerals are smectites. Electron microprobe analysis (see previous section) has shown that the smectites were dominantly of trioctahedral compositions (saponites and Al-saponites), but no estimate could be made of the proportions of smectite to chlorite. Viereck et al. (1986) reported that chlorite-smectite was common in Hole 585 volcanoclastics, but without supporting X-ray powder diffraction evidence. Reynolds (1980) calculated diffraction patterns for randomly and fully ordered interstratified trioctahedral chlorite-trioctahedral smectites. The smectites from Leg 129 volcanoclastics have no diffraction peak at 31 \AA , so they cannot be fully ordered, but are randomly interstratified. The d(001) (glycolated) varies between 16.7–17.0 \AA (except for one sample) suggesting <10% chlorite as an interlayered component.

There are several zeolite minerals indicated by the X-ray patterns (Table 3 on microfiche), including clinoptilolite and phillipsite, and less commonly, analcite. Clinoptilolite is the dominant zeolite in the Cretaceous volcanoclastics, whereas phillipsite is more common in the Miocene. The presence of phillipsite is thought to be restricted to marine sediments younger than mid-Cretaceous (Kastner, 1981).

Opal-CT is present in several of the volcanoclastic horizons in the Cretaceous and has been identified by a broad diffraction maximum at about 4.10 \AA . Calcite is present throughout the whole sequence of the volcanoclastics both as bioclastic material and sometimes as a fine-grained, groundmass mosaic. It is often a secondary replacement for clay minerals, but may also pseudomorph primary crystal fragments such as olivine and plagioclase.

CHEMISTRY OF THE VOLCANICLASTITES

The bulk chemistry of 73 volcanoclastic samples are presented in Table 4 (Site 800, Unit IV), Table 5 (Site 801, Unit III, and Site 802, Units V and VIII–IX), and Table 6 (Site 802, Unit II, Miocene), all on microfiche in the back of this volume. It can be seen from these tables that the loss on ignition (LOI) value of most samples is very high (range: 1.96 to 27.7 wt%), reflecting in large part the hydration of the glassy fragments during argillization. Since these high volatile contents can have a serious distorting effect on any chemical trends, all the analyses have been recalculated to a volatile-free basis (listed in Appendixes A, B, and C on microfiche in the back of this volume). These values have been used in all the geochemical diagrams and are denoted by the superscript asterisk (*) adjacent to each element. Separate values for H₂O⁺ and CO₂ were not determined.

Interpretation Problems

The bulk chemistry of volcanoclastic sediments represents an integration of various components derived from a variety of different sources. These components may include: volcanic rocks of both submarine and subaerial origin from one or more eruptive sites and possibly from different eruptive episodes, biogenic material, such as microfossil tests and reefal debris, and terrigenous clays derived by wind or oceanic currents from adjacent continental masses. The resultant geochemical signature may, thus, be more difficult to interpret relative to lavas, where secondary processes are the main factor in modifying the initial magmatic signature. Secondary alteration, due to the effects of seawater interaction, can also have a modifying effect on the volcanoclastites, especially during the argillization of glass. Low-grade, hydrous alteration of glass (and bulk rock) causes variation in the contents of the more mobile elements (K, Rb, Ba, Sr) and the loss of coherence between the ratios of these elements (for example, Hart et al., 1974, Humphris and Thompson, 1978).

To a first approximation, if the volcanogenic sediments represent reworked, altered hyaloclastites, the chemical data can be treated and interpreted in a similar fashion to basalt lavas—the hyaloclastites being accumulations of basaltic glass. However, an additional problem arises due to the diluting effects of siliceous and calcareous materials, even after the “removal” of volatile constituents. However, while the diluents have simple compositions (SiO₂, CaCO₃) they do not reduce the identification of the igneous source characteristics significantly, as their effect on magmatic trends can be readily determined in simple chemical diagrams. For example, as seen in Figure 7, silicified samples lie on a mixing line between SiO₂ and the centroid of the data set (Fig. 7A) and calcareous samples define a mixing path to the CaO apex (Fig. 7B).

Chemical Variation with Depth

The variation in composition with depth at each site for selected elements is illustrated in Figures 8 to 10, and exhibit a number of different patterns. At Site 800 (Fig. 8) the large amplitude of scatter above 280 mbsf, for both major oxides and trace elements reflects variable dilution by nonvolcanogenic siliceous material and minor calcareous debris. Lower down in the sequence the pattern becomes much more coherent for stable trace elements (Zr, Y, Nb) and their ratios, whereas mafic elements (MgO, Cr, and Ni) show a steady increase with depth. The trends for Site 801 (Fig. 9), with a very much less dense sampling interval, are more erratic with an apparent peaking of mafic element abundances (and Ti, Zr) around the middle of the succession. Due to the paucity of data for the Cretaceous succession at Site 802 (Fig. 10) no meaningful trends are displayed. The Miocene succession, however, shows a slight increase in stable incompatible elements (Ti, Nb, Y, and possibly Zr) with height, although this could be the function

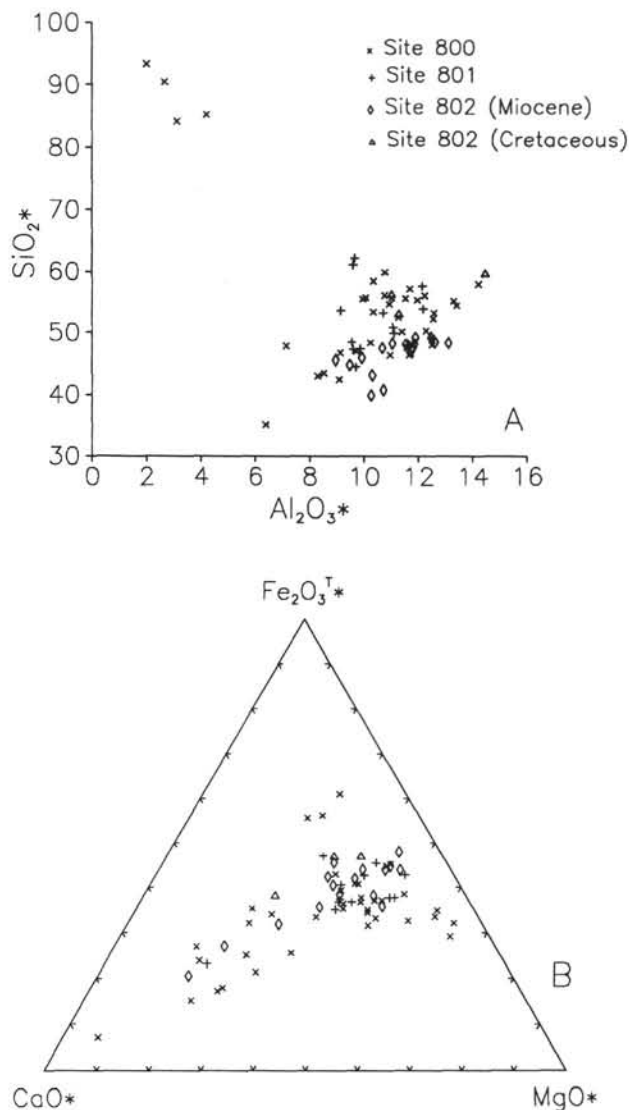


Figure 7. Effects of nonvolcanogenic components, silica (A) and carbonate (B), on the bulk chemical composition of volcanoclastite samples from Sites 800, 801, and 802.

of dilution by calcareous material in the basal portion (with high CaO). Mafic elements (Mg, Ni, Cr) behave in a coherent fashion and show a crude, erratic, decrease with height, above the central part of the sequence.

Magmatic Affinity and Tectonic Setting

Because of the effects of dilution and alteration, ratios of the more stable incompatible elements (Ti, Zr, Y, Nb) are better indicators of any systematic changes throughout the volcanoclastic sequences that might reflect variable source composition or magma type. Although ratios such as Cr*/Ni*, Zr*/Y* and Zr*/Nb* (Figs. 8, 9, and 10), are slightly variable throughout all sites, they do not show any marked chemical hiatus with depth, with the possible exception of the Cretaceous of Site 801 at about 190 mbsf. All the Cretaceous volcanoclastites have relatively compatible ratios of these elements and generally overlapping compositions. It is inferred, therefore, that their various sources were not only similar, but remained essentially constant in terms of the broad composition of basaltic components being supplied to the deep basins.

The main difference between the volcanoclastite suites is that the Miocene sediments exhibit generally higher Zr*/Y* and Zr*/Nb* ratios, although many other elements show a similar compositional range as the Cretaceous volcanoclastites. The Miocene volcanoclastites are alkaline in chemical composition and have been derived from fragmented alkali basalts—a feature also suggested by the composition of their crystal fragments (see previously). They are comparable with alkali basalt clasts from Site 585 in the Eastern Mariana Basin (Viereck et al., 1986; Floyd, 1986a) which have similar incompatible element ratios. The Cretaceous volcanoclastites are also broadly alkaline in composition, but trend to a more transitional basalt character as shown by the wide range of incompatible element abundances and lower ratios (for example, Site 800).

Absolute abundances and ratios of stable incompatible elements in both the Cretaceous and Miocene volcanoclastites fall within the range of "within-plate" ocean island basalts, as would be expected from their environmental setting (see below). Zr/Y ratios are high in the vitric-rich volcanoclastites and fall towards the top of the 4 to 11 range, generally considered typical of within-plate, alkaline environments (Pearce and Norry, 1979). Similarly, the Ti/V ratio can be used to discriminate magma type and tectonic setting (Sherrais, 1982), with variable ratios for within-plate transitional seamount basalts (40 to 50) and ocean island alkali basalts (50 to 110). Ti/V ratios for the Cretaceous volcanoclastites range from 45 (Site 800) to 66 (Site 802), and 54 for the Miocene samples at Site 802.

In eruptive environment discrimination diagrams (for example, Pearce and Cann, 1973; Pearce et al., 1977; Meschede, 1986), both the Cretaceous and Miocene volcanoclastites largely plot in the "within-plate" designated field. In the Zr-Nb-Y diagram (Fig. 11), however, the scatter exhibited emphasizes the apparent alkaline to transitional magmatic character of the Cretaceous source lavas. The Miocene volcanoclastites plot in a tight group relative to the Cretaceous sediments, which may reflect the latter having been derived from more varied sources (many seamounts in different basins?) compared to the (single source?) Miocene.

ORIGIN AND SOURCE OF VOLCANICLASTITES

In this section we shall briefly consider the original environment within which the volcanogenic material was generated and the nature of the source material available. Interpretation of seismic profiles and correlation with drilled sections suggests that much of the floor of the western Pacific may be carpeted with volcanoclastites of mid-Cretaceous age (Winterer, 1973; Schlanger et al., 1981; Schlanger and Moberly, 1986). For example, sites in the Mariana Basin, such as Hole 585 (Moberly, Schlanger, et al., 1986), encountered thick, mid-Cretaceous, turbiditic volcanoclastites, which are generally considered to have been shed from the debris covered flanks of adjacent seamounts of similar age. Sedimentological evidence indicates that the Cretaceous and Miocene volcanoclastite units drilled during Leg 129 were deposited via mass flow mechanisms and represent both distal and proximal turbidites and debrites (Lancelot, Larson, et al., 1990). The morphological, petrographic and chemical features of the volcanoclastites and their clasts (detailed previously), provide some evidence as to their initial environment prior to redeposition.

The primary magmatic characters exhibited by the various clasts within the Cretaceous volcanoclastites can be summarized as follows: (1) there is a preponderance of vesicular glass shards with both angular and cusped margins, (2) quench-textured and holocrystalline lithic fragments are basalts, (3) the chemical features of large crystal fragments (phenocrysts released from their matrix) are typical of those crystallizing from alkalic basalt magmas, and (4) the bulk chemistry of highly vitric units is similar to alkaline basaltic sequences characteristic of the within-plate, ocean-island eruptive environment. These general features apply to the Miocene volcanoclastites as well, there being little major difference between them. The proportions of vitric to lithic clasts in the volcanoclastites,

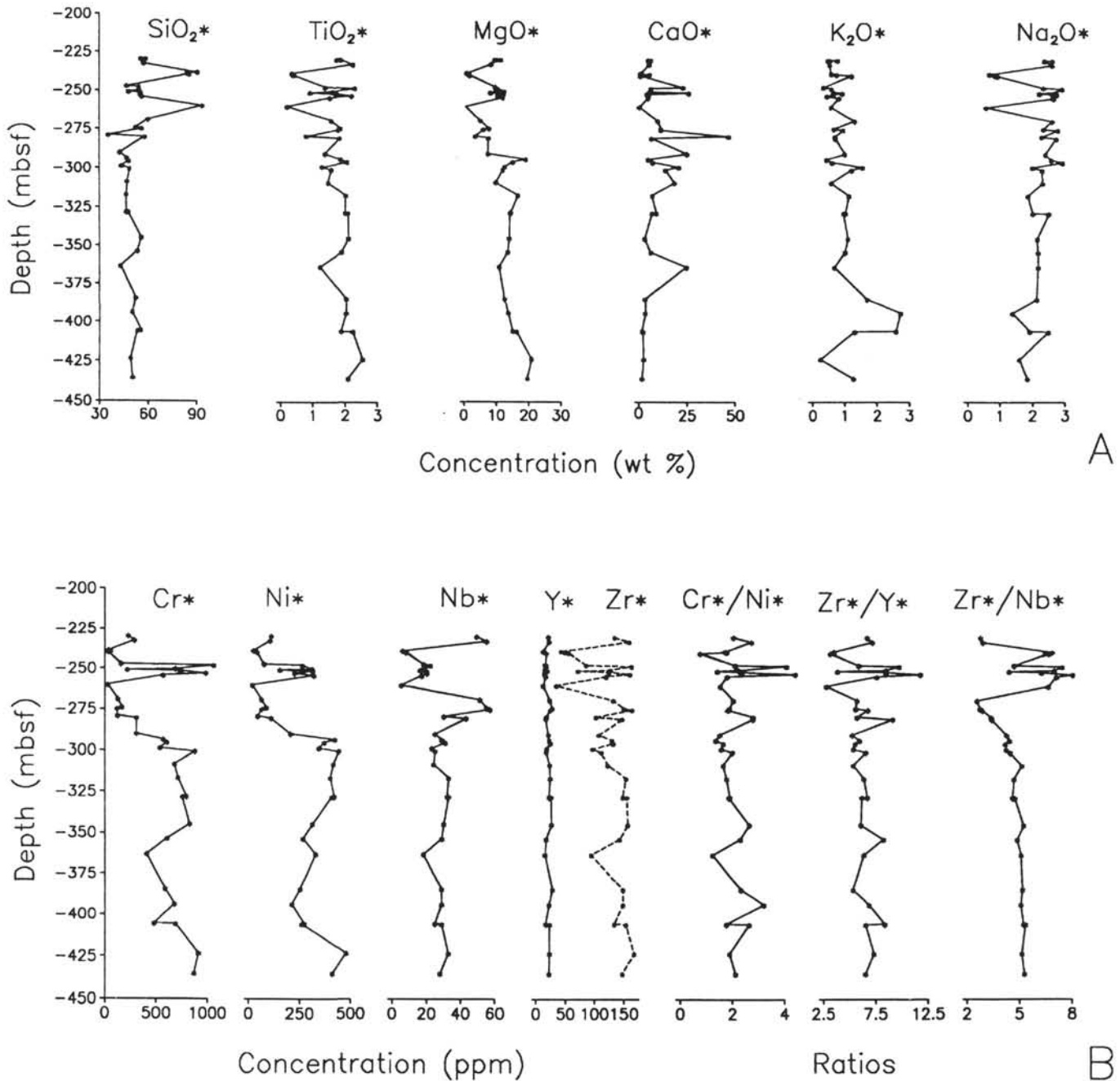


Figure 8. Distribution of major oxides (A) and trace elements and their ratios (B), relative to stratigraphic depth in Site 800 volcaniclastites.

and the shapes of glass shards, are typical of hyaloclastite deposits formed subaqueously by the interaction of hot magma and cold seawater (McBirney, 1971; Honnorez and Kirst, 1975; Bonatti and Harrison, 1988). We consider, therefore, that both the Cretaceous and Miocene volcaniclastites are largely representative of turbidity current redeposited hyaloclastites derived from an alkaline basalt dominated source.

Eruptive Environment and Reworking of Hyaloclastites

Hyaloclastites can be formed via three main processes: rapid vesiculation, spalling of pillow lava rims, and direct quench granulation, although the first process would only take place at relatively shallow depths (<500 m) where hydrostatic pressures were low (Fisher and Schmincke, 1984). At relatively shallow depths steam

explosivity may be an additional process that can also produce shards (Kokelaar, 1986). Highly vitric deposits can form at various water depths and have been recorded in a number of deep-sea environments. For example, hyaloclastites have been found interbedded with pillow basalts from spreading centers (Schmincke et al., 1978) and as talus flows associated with the calderas of near-ridge seamounts (Lonsdale and Batiza, 1980; Batiza et al., 1984; Fornari et al., 1984). In the latter case, seamount hyaloclastites consist of blocky and platy shards formed *in situ* by the rapid granulation of a submarine lava fountain eruption (Smith and Batiza, 1989). Rapid eruption rate promotes the formation of clastic deposits relative to lava flows at high hydrostatic pressures (or in deep water). In some cases a slurry of shards, steam, and seawater might form an unstable density current which carries particles away and redeposits them a short distance down slope from the original vent (Smith and Batiza, 1989).

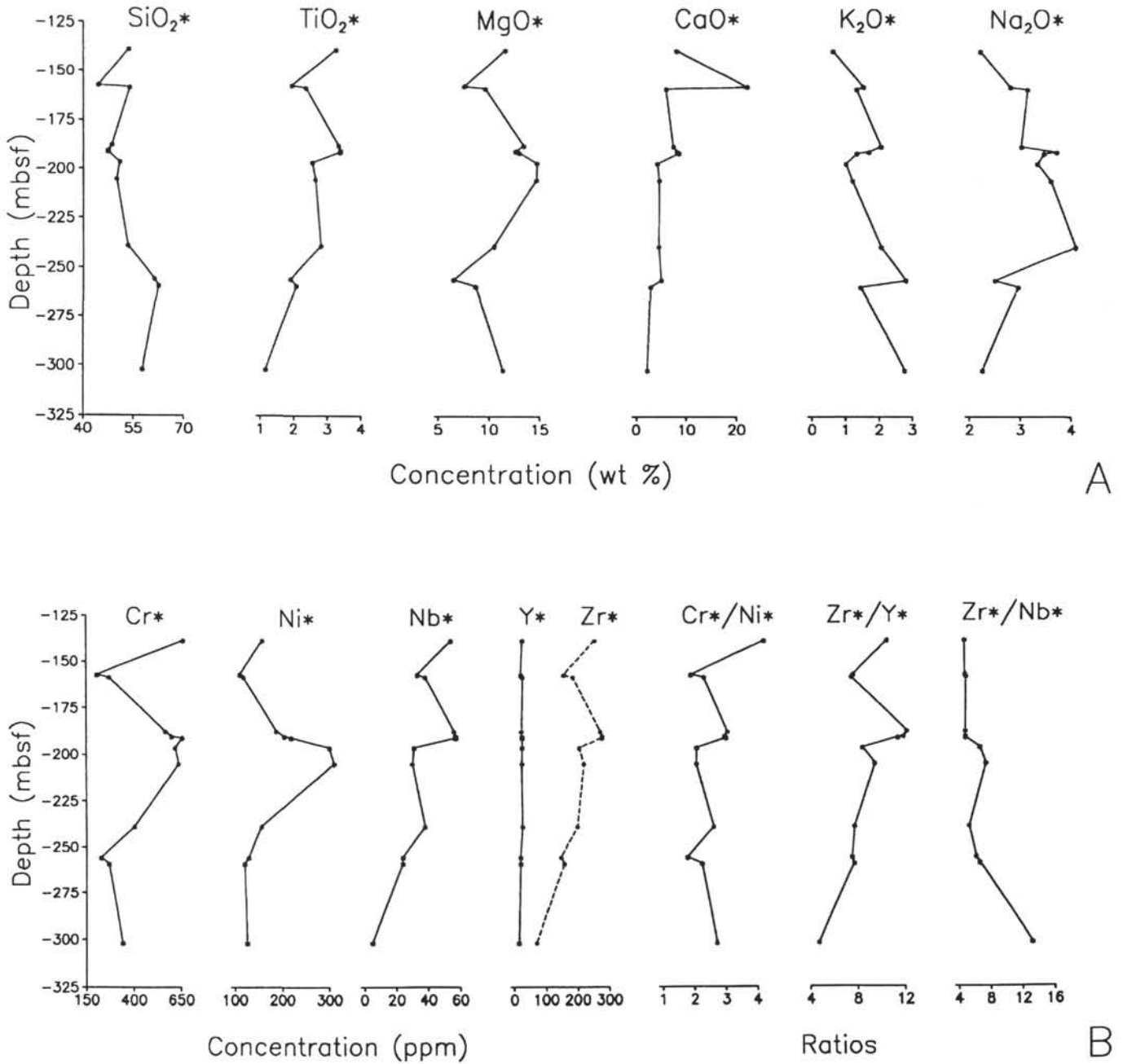


Figure 9. Distribution of major oxides (A) and trace elements and their ratios (B), relative to stratigraphic depth in Site 801 volcaniclastites.

It is, however, the relatively shallow-water environment, adjacent to ocean islands or associated with nearly emergent seamounts, that provides the greatest scope for the production of volcaniclastites and their subsequent reworking via mass wasting processes. As seamounts build up to sea level explosive activity predominates over submarine lava flow production with the development of an extensive clastic carapace that may extend as an apron beyond the volcanic edifice (Moore and Fiske, 1969; Furnes and Sturt, 1976; Fisher and Schmincke, 1984; Staudigel and Schmincke, 1984). Due to the gravitational instability and mass wasting of such volcaniclastic deposits, huge submarine slumps and debris avalanches may transport them down to fill the flexural moats surrounding oceanic islands such as Hawaii (Moore, 1964; Lipman et al., 1988; Moore et al., 1989). Debris avalanches reported on the Hawaiian Ridge (off Oahu) can reach over 200 km long, traversing the moat, but not apparently extending beyond the present upwarped Hawaiian Arch. Slope failure may begin

early in the life of an oceanic volcano (as a small seamount), although culminates during the subaerial stage when the volcano is a few kilometers above sea level (Moore et al., 1989). Earthquakes are considered to be the trigger mechanism for mass wasting on continental slopes (for example, Kenyon, 1987), whereas microseismic pulses in volcanic ocean islands would be related to explosive activity, magma transport and rift development.

In summary, the shallow-water environment surrounding oceanic volcanoes is not only conducive to the production of abundant volcaniclastites, but one from which mass wasting could transport large quantities of volcanogenic materials into the surrounding deep basins. Schematic models of sedimentary facies around oceanic volcanoes suggest turbidite flows carry material well beyond the emerging seamount or ocean island to eventually produce a mixed facies of volcanogenic, pelagic and shallow reefal components (for example, Kelts and Arthur, 1981; Batiza and Watts, 1986; Cas and Wright, 1987).

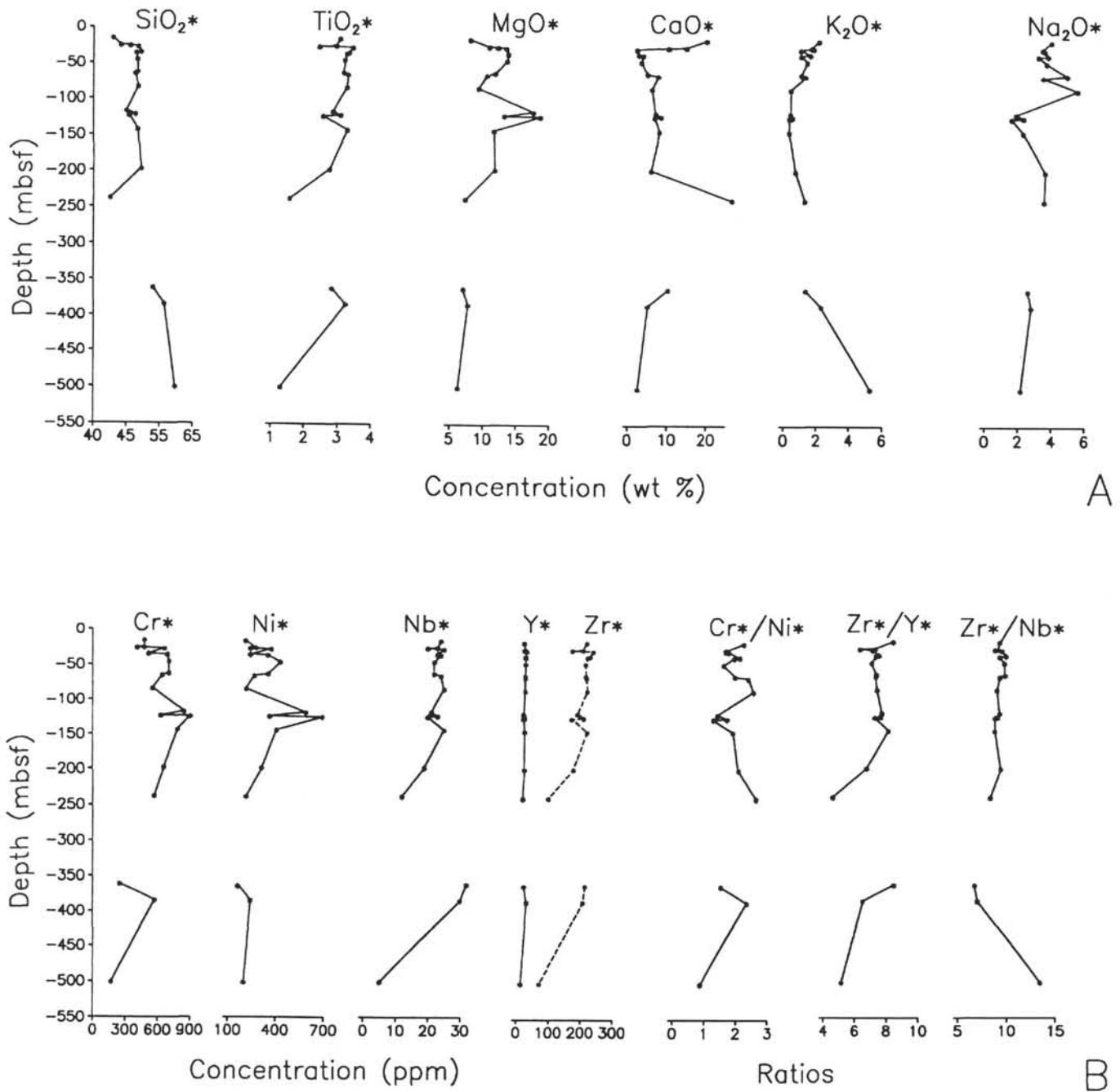


Figure 10. Distribution of major oxides (A) and trace elements and their ratios (B), relative to stratigraphic depth in Site 802 volcaniclastites.

Sources of Mid-Cretaceous and Miocene Volcaniclastites

Due to the overall similarities of the primary features exhibited by both mid-Cretaceous and Miocene volcanogenic sediments, they will be initially considered together. The nature of the vitric clasts suggests they were originally derived from hyaloclastite accumulations. Various additional features indicate that the volcanic activity which produced them was generated in a shallow-water environment adjacent to a reef-fringed, emergent (or near emergent) volcanic island(s). In particular, the highly vesicular nature of the glass shards and the associated, quench-textured, basalt clasts indicates a shallow-water depth of possibly a few hundreds of meters. However, as the original lavas were volatile-rich alkalic basalts (relative to tholeiites), vesiculation could have taken place at greater depths, down to a maximum of about 1800 m (about 500 m for tholeiites). However, nonvolcano-

genic materials incorporated into the hyaloclastite debris flows provide additional evidence for a shallow-water environment: the presence of (1) ooids, some having grown on a basaltic core, (2) reefal debris and typical shallow-water fauna, and (3) glauconite pellets. Rare wood fragments and spores found within the Hole 802A Aptian-Albian volcaniclastic succession implies that their source region was probably emergent. Similarly, the occasional presence of tubular scoriae and clasts with multichambered, irregular vesicles could imply a contribution from a subaerial source for all successions.

From a consideration of the nature and formation of volcaniclastites given above, Leg 129 hyaloclastites were mainly derived from a shallow-water eruptive setting around emergent oceanic volcanoes and carried to their present position via slumping probably triggered by volcanic activity. The actual sources for the volcanogenic sediments must be present among the seamounts and ocean islands of

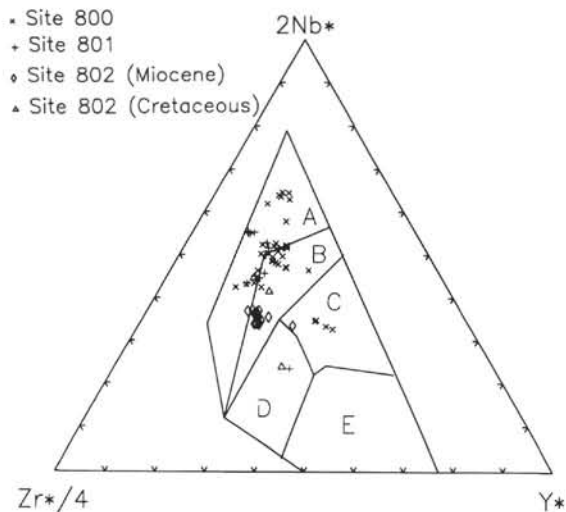


Figure 11. Chemical discrimination of the original eruptive environment of basalt lava-derived volcanoclastites. Tectonic fields (from Meschede, 1986) are: A = within-plate (alkaline-dominated), B = within-plate (alkaline and tholeiitic), C = plume-type MORB, D = volcanic arc, and E = normal-type MORB and volcanic arc.

similar age in the general vicinity of the Pigafetta and Mariana basins (Lancelot, Larson, et al., 1990).

Site 800 volcanoclastites are mainly Aptian in age and could have been derived from one or all of three nearby seamounts of Cretaceous age (Fig. 12): Himu Seamount (65 km to the southwest), Golden Dragon guyot (160 km to the southeast), or an unnamed guyot further away to the northeast. The volcanoclastites are broadly alkaline in composition, similar to Himu and Golden Dragon, and the deep-sea dolerite sills also encountered in Hole 800A (Floyd et al., this volume). The mainly Albian volcanoclastites of Site 801 are again alkaline; their nearest probable sources being seamounts about 150–180 km to the north and south. The sources for Site 802 are more problematic, sampling both Aptian-Albian and Coniacian-Campanian volcanoclastites, and being situated in an apparently seamount-free portion of the Mariana Basin (Fig. 12). Although seamounts which fringe the Mariana Basin to the north and east are possible source areas (about 300 km away), drilling at Sites 199 and 585 to the east only encountered the older group of Cretaceous volcanoclastites which were clearly derived from a local source such as Ita Maitai guyot (Moberly, Schlanger, et al., 1986).

Most intriguing of all is the source region for the Miocene volcanoclastites from Site 802, being a deep-water location well away from any known seamounts of Tertiary age. The nearest Miocene volcanic activity is recorded in the submarine ridge containing the Eastern Caroline Islands, some 350 km to the south (Lancelot, Larson, et al., 1990). Truk is the only island within the chain to be a possible source, with lavas old enough (10.9 Ma; Keating et al., 1984), and exhibiting a chemical composition (Truk Main Lava Series; Matthey, 1982), not dissimilar to the Miocene volcanoclastites. Because of the hyaloclastic nature of the sediments, mixed with shallow-water faunal debris and rip-up clasts of bedded tuffs, they were probably derived from Truk's submarine platform and then transported northwards by exceptional vigorous turbidity currents.

COMMENTS AND CONCLUSIONS

1. Mid-Cretaceous volcanoclastite sequences were sampled in the Pigafetta and Mariana basins at Sites 800, 801, and 802. In addition, Miocene volcanoclastites were obtained from the upper units of Site 802. The remarkable point about them is the striking resemblance they bear to one another in terms of the texture, petrology, and chemistry of their

constituent clasts and the bulk rock; any differences are comparably minor. This convergence of features suggests they have been produced essentially from the same types of source materials and by the same mechanisms. They also exhibit features similar to mid-Cretaceous volcanoclastites described from Site 585 in the East Mariana Basin (Floyd, 1986a, 1986b; Viereck et al., 1986), with the exception that the latter contains evidence for both tholeiitic and alkali basalt precursors, and that the vesicles are uniformly small and spherical.

2. In the volcanoclastites, all the igneous lithic material is basaltic in composition, ranging from glassy to holocrystalline fragments, which may be variably olivine-, clinopyroxene-, and plagioclase-phyric. Most vitric components are replaced by palagonite and finally by varieties of smectite; fresh sideromelane is preserved in the Miocene volcanoclastites. The composition of fragmental crystal material (diopsidic and augitic pyroxene, basic plagioclase, olivine, and rare titaniferous pargasite and biotite), seen throughout most of the volcanoclastite sequences, are typical of phases that crystallize from differentiated, hydrous, alkalic basalt melts. Because of its relative resistance to alteration, clinopyroxene is ubiquitous, whereas fresh olivine is only seen in the Miocene sediments. Fine-grained, laminated, tuffaceous clasts form an important component in the upper units of Site 802, and probably represent rip-ups from partly consolidated water-lain ashes on the seafloor. In the more altered sediments a large component comprises a structureless smectite matrix which has been largely derived by the degradation of fine-grained glass particles initially deposited as ash. Nonvolcanogenic components are mainly secondary carbonate, ooids, and biogenic reefal material, indicative of derivation from a shallow-water environment.

3. The bulk chemistry of the volcanoclastites is relatively uniform and within the limits of sampling, no major chemical breaks with depth are recorded throughout each sequence. Abundances and ratios of stable incompatible elements indicate that the volcanoclastites have been derived from a series of predominantly alkali to transitional basalts characteristic of the "within-plate" or ocean-island eruptive environment. The much more restricted chemical composition exhibited by the Miocene volcanoclastites, relative to their Cretaceous analogues, may reflect derivation from a single rather than a multiple source.

4. Secondary alteration of the volcanoclastites is dominated by aluminous smectites with variable Fe/Mg ratios (depending on the host replaced), celadonite, carbonates, zeolites (phillipsite, clinoptilolite), and silica. Apart from some sideromelane in the Miocene, all glass is replaced by either palagonite or brownish smectites. The intimate mixing of both fresh and variably altered material implies that much of the alteration took place at source rather than at the site of final deposition. The secondary assemblages are characteristic of the low-temperature zeolite facies and developed under poorly oxidizing conditions.

5. Regarding the source and origin of present-day volcanoclastite flows, it is considered that the Leg 129 volcanogenic sediments were emplaced as a series of turbidite and debris flows from the slopes of adjacent seamounts and/or oceanic islands. The occurrence of highly vesicular basaltic glass and clasts, carbonate ooids, and reef debris in both Miocene and Cretaceous sequences suggests that the mass flow source region was located in shallow water. The highly vitric nature and bulk composition of the sediments indicates they were originally accumulations of hyaloclastic material generated in shallow water by the reaction of alkali basalt lava with seawater. A component of subaerial volcanic material (possibly represented by water-lain laminated tuffs) and now included as rounded, rip-up clasts was probably low. The discovery of wood fragments in the Miocene of Site 802 suggests that the source region for that sequence was almost certainly emergent.

ACKNOWLEDGMENTS

Thanks are due to Leg 129 shipboard colleagues for comments on the sedimentary character and origin of the volcanoclastites. The bulk

rock chemical analyses were determined at the University of Keele (Geoscience Analytical Services) with the able help of David Emley and Margaret Aikin. Electron microprobe analyses were performed at the Geology Department, University of Manchester, and we are grateful to Professor C. D. Curtis for permission to use the instruments, and to Tim Hopkins and Dave Plant for skilled assistance. Ralph Moberly and an unknown reviewer are thanked for their comments which tidied up the initial manuscript considerably.

REFERENCES

- Adamson, A. C., 1981. Chemistry of alteration minerals from Deep Sea Drilling Project Sites 501, 504 and 505. *In* Cann, J. R., Langseth, M. G., Honnorez, J., Von Herzen, R. P., White, S. M., et al., *Init. Repts. DSDP*, 69: Washington (U.S. Govt. Printing Office), 551–563.
- Batiza, R., Fornari, D. J., Vanko, D. A., and Lonsdale, P., 1984. Craters, calderas and hyaloclastites on young Pacific seamounts. *J. Geophys. Res.*, 89:8371–8390.
- Batiza, R., and Watts, A. B., 1986. Scientific seamount drilling report. *JOI-USSAC sponsored workshop*, Lamont-Doherty Geological Observatory, 1–13.
- Bonatti, E., and Harrison, C.G.A., 1988. Eruption styles of basalt in oceanic spreading ridges and seamounts: effect of magma temperature and viscosity. *J. Geophys. Res.*, 93:2967–2980.
- Bowles, F. A., Jack, R. N., and Carmichael, I.S.E., 1973. Investigation of deep-sea volcanic ash layers from Equatorial Pacific cores. *Geol. Soc. Am. Bull.*, 84:2371–2388.
- Cas, R.A.F., and Wright, J. V., 1987. *Volcanic Successions—Modern and Ancient*: London (Allen and Unwin).
- Dunham, A. C., and Wilkinson, F.C.F., 1978. Accuracy, precision and detection limits of energy-dispersive electron microprobe analysis of silicates. *X-Ray Spectrom.*, 7:50–56.
- Fisher, R. V., and Schmincke, H.-U., 1984. *Pyroclastic Rocks*: Berlin (Springer-Verlag).
- Floyd, P. A., 1986a. Geochemistry and provenance of basaltic clasts within volcanoclastic debris flows, East Mariana Basin, Deep Sea Drilling Project Site 585. *In* Moberly, R., Schlanger, S. O., et al., *Init. Repts. DSDP*, 89: Washington (U.S. Govt. Printing Office), 449–458.
- , 1986b. Glassy and basaltic fragments within graded volcanoclastic sediments, East Mariana Basin, Deep Sea Drilling Project Leg 89. *In* Moberly, R., Schlanger, S. O., et al., *Init. Repts. DSDP*, 89: Washington (U.S. Govt. Printing Office), 433–447.
- Floyd, P. A., and Rowbotham, G., 1986. Chemistry of primary and secondary phases in intraplate basalts and volcanoclastic sediments, Deep Sea Drilling Project Leg 89. *In* Moberly, R., Schlanger, S. O., et al., *Init. Repts. DSDP*, 89: Washington (U.S. Govt. Printing Office), 459–469.
- Fornari, D. J., Ryan, W.B.F., and Fox, P. J., 1984. The evolution of craters and calderas on young seamounts: insights from SeaMARC-1 and Seabeam sonar surveys of a small seamount group near the axis of the East Pacific Rise at 10°N. *J. Geophys. Res.*, 89:11069–11083.
- Furnes, H., and Sturt, B. A., 1976. Beach/shallow marine hyaloclastite deposits and their geological significance—an example from Gran Canaria. *J. Geol.*, 84:439–453.
- Haggerty, J. A., Schlanger, S. O., and Premoli-Silva, I., 1982. Late Cretaceous and Eocene volcanism in the southern Line Islands and implications for hotspot theory. *Geology*, 10:433–437.
- Hart, S. R., Erlank, A. J., and Kable, E.J.D., 1974. Sea floor basalt alteration: some chemical and Sr isotopic effects. *Contrib. Mineral. Petrol.*, 44:219–230.
- Henderson, C.M.B., and Gibb, F.G.F., 1988. The petrology of the Lugar Sill, S.W. Scotland. *Trans. R. Soc. Edinburgh*, 77:325–347.
- Honnorez, J., 1981. The aging of the oceanic lithosphere. *In* Emiliani, C. (Ed.), *The Sea* (Vol. 7): *The Oceanic Lithosphere*: New York (Pergamon Press), 525–567.
- Honnorez, J., and Kirst, P., 1975. Submarine basaltic volcanism: morphologic parameters for discriminating hyaloclastites from hyalotuffs. *Bull. Volcanol.*, 39:1–25.
- Houghton, R. L., 1979. Petrology and geochemistry of basaltic rocks recovered on Leg 43 of the Deep Sea Drilling project. *In* Tucholke, B. E., Vogt, P. R., et al., *Init. Repts. DSDP*, 43: Washington (U.S. Govt. Printing Office), 721–738.
- Humphris, S. E., and Thompson, G., 1978. Hydrothermal alteration of oceanic basalts by seawater. *Geochim. Cosmochim. Acta*, 42:107–126.
- Kastner, M., 1981. Authigenic silicates in deep-sea sediments: formation and diagenesis. *In* Emiliani, C. (Ed.), *The Sea* (Vol. 7): *The Oceanic Lithosphere*: New York (Pergamon Press), 915–980.
- Keating, B. H., Matthey, D. P., Naughton, J., and Helsley, C. E., 1984. Age and origin of Truk Atoll, Eastern Caroline Islands: geochemical, radiometric age and palaeomagnetic evidence. *Geol. Soc. Am. Bull.*, 95:350–356.
- Kelts, K., and Arthur, M. A., 1981. Turbidities after ten years of deep sea drilling—wringing out the mop? *In* Warme, J. E., Douglas, R. G., and Winterer, E. L. (Eds.), *The Deep Sea Drilling Project—a Decade of Progress*. Spec. Publ.—Soc. Econ. Paleontol. Mineral., 32:91–127.
- Kenyon, N. H., 1987. Mass-wasting features on the continental slope of northwest Europe. *Mar. Geol.*, 74:57–77.
- Kokelaar, B. P., 1986. Magma-water interactions in subaqueous and emergent basaltic volcanics. *Bull. Volcanol.*, 48:275–290.
- Lancelot, Y., Larson, R. L., et al., 1990. *Proc. ODP, Init. Repts.*, 129: College Station, TX (Ocean Drilling Program).
- Larson, R. L., 1991. Latest pulse of Earth: evidence for a mid-Cretaceous superplume. *Geology*, 19:547–550.
- Larson, R. L., and Schlanger, S. O., 1981. Geological evolution of the Nauru Basin and regional implications. *In* Larson, R. L., Schlanger, S. O., et al., *Init. Repts. DSDP*, 61: Washington (U.S. Govt. Printing Office), 841–862.
- Leake, B. E., 1978. Nomenclature of amphiboles (for subcommittee on amphiboles, IMA). *Mineral. Mag.*, 42:533–563.
- Lipman, P. W., Normark, W. R., Moore, J. G., Wilson, J. B., and Gutmacker, C. E., 1988. The giant submarine Alika debris slide, Maura Loa, Hawaii. *J. Geophys. Res.*, 93:4279–4299.
- Lonsdale, P., and Batiza, R., 1980. Hyaloclastite and lava flows on young seamounts examined with a submersible. *Geol. Soc. Am. Bull.*, 91:545–554.
- Matthey, D. P., 1982. The minor and trace element geochemistry of volcanic rocks from Truk, Ponape and Kusaie, Eastern Caroline Islands: the evolution of a young hot spot trace across old Pacific Ocean crust. *Contrib. Mineral. Petrol.*, 80:1–13.
- McBimney, A. R., 1971. Oceanic volcanism: a review. *Rev. Geophys. Space Phys.*, 9:523–556.
- Meschede, M., 1986. A method of discriminating between different types of mid-ocean ridge basalts and continental tholeiites with the Nb-Zr-Y diagram. *Chem. Geol.*, 56:207–218.
- Moberly, R., Schlanger, S. O., et al., 1986. *Init. Repts. DSDP*, 89: Washington (U.S. Govt. Printing Office).
- Moore, J. G., 1964. Giant submarine landslides on the Hawaiian Ridge. *Geol. Surv. Prof. Pap. U.S.*, 501-D:95–98.
- Moore, J. G., Clague, D. A., Holcomb, R. T., Lipman, P. W., Normark, W. R., and Torresan, M. E., 1989. Prodigious submarine landslides on the Hawaiian Ridge. *J. Geophys. Res.*, 94:17465–17484.
- Moore, J. G., and Fiske, R. S., 1969. Volcanic substructure inferred from dredge samples and ocean-bottom photographs, Hawaii. *Geol. Soc. Am. Bull.*, 80:1191–1201.
- Pearce, J. A., and Cann, J. R., 1973. Tectonic setting of basic volcanic rocks determined using trace element analyses. *Earth Planet. Sci. Lett.*, 19:290–300.
- Pearce, J. A., and Norry, M. J., 1979. Petrogenetic implications of Ti, Zr, Y and Nb variations in volcanic rocks. *Contrib. Mineral. Petrol.*, 69:33–47.
- Pearce, T. H., Gorman, B. E., and Birkett, T. C., 1977. The relationship between major element chemistry and tectonic environment of basic and intermediate volcanic rocks. *Earth Planet. Sci. Lett.*, 36:121–132.
- Rea, D. K., and Vallier, T. L., 1983. Two Cretaceous volcanic episodes in the western Pacific Ocean. *Bull. Geol. Soc. Am.*, 94:1430–1437.
- Reynolds, R. C., 1980. Interstratified clay minerals. *In* Brindley, G. W., and Brown, G. (Eds.), *Crystal Structures of Clay Minerals and their X-ray Identification*. Mineral. Soc. London Monogr., 5:249–303.
- Scheidegger, K. P., Jezek, P. A., and Shackleton, D., 1978. Chemical and optical studies of glass shards in Pleistocene and Pliocene ash layers from DSDP Site 192, northwest Pacific Ocean. *J. Volcanol. Geotherm. Res.*, 4:99–116.
- Schlanger, S. O., Jenkyns, H., and Premoli-Silva, I., 1981. Volcanism and vertical tectonics in the Pacific basin related to global Cretaceous transgressions. *Earth Planet. Sci. Lett.*, 52:435–449.
- Schlanger, S. O., and Moberly, R., 1986. Sedimentary and volcanic history: East Mariana Basin and Nauru Basin. *In* Moberly, R., Schlanger, S. O., et al., *Init. Repts. DSDP*, 89: Washington (U.S. Govt. Printing Office), 653–678.
- Schmincke, H.-U., 1981. Ash from vitric muds in deep sea cores from the Mariana Trough and Fore-Arc region (South Philippine Sea) (Sites 453, 454, 455, 458, 459 and SP), Deep Sea Drilling Project, Leg 60. *In* Hussong, D. M., Uyeda, S., et al., *Init. Repts. DSDP*, 60: Washington (U.S. Govt. Printing Office), 473–481.
- , 1983a. Ash layers, hyaloclastite and alteration of basalt glass, Leg 65. *In* Lewis, B. T., Robinson, P. T., et al., *Init. Repts. DSDP*, 65: Washington (U.S. Govt. Printing Office), 477–483.

- , 1983b. Rhyolitic and basaltic ashes from the Galapagos Mounds area, Leg 70, Deep Sea Drilling Project. In Cann, J. R., Langseth, M. G., Honnorez, J., Von Herzen, R. P., White, S. M., et al., *Init. Repts. DSDP*, 69: Washington (U.S. Govt. Printing Office), 451–457.
- Schmincke, H.U., Robinson, P. T., Ohnmacht, W., and Flower, M. J. F., 1978. Basaltic hyaloclastites from Hole 396B DSDP Leg 46. In Dmitriev, L., Heirtzler, J., et al., *Init. Repts. DSDP*, 46: Washington (U.S. Govt. Printing Office), 341–346.
- Schmincke, H.-U., Viereck, L. G., Griffin, B. J., and Pritchard, R. G., 1982. Volcaniclastic rocks of the Reydarfjordur Drill Hole, eastern Iceland. 1: Primary features. *J. Geophys. Res.*, 87:6437–6458.
- Shervais, J. W., 1982. Ti-V plots and the petrogenesis of modern and ophiolitic lavas. *Earth Planet. Sci. Lett.*, 59:101–118.
- Smith, T. L., and Batiza, R., 1989. New field and laboratory evidence for the origin of hyaloclastite flows on seamount summits. *Bull. Volcanol.*, 51:96–114.
- Staudigel, H. R., and Hart, S. R., 1983. Alteration of basaltic glass: mechanism and significance for the oceanic crust-sea water budget. *Geochim. Cosmochim. Acta*, 47:337–350.
- Staudigel, H. R., and Schmincke, H.-U., 1984. The Pliocene seamount series of La Palma/Canary Islands. *J. Geophys. Res.*, 89:11195–11215.
- Velde, B., 1985. *Clay Minerals—a Physico-chemical Explanation of Their Occurrence*. Amsterdam (Elsevier), Dev. in Sedimentol. Ser., 40.
- Viereck, L. G., Griffin, B. J., Schmincke, H.-U., and Pritchard, R. G., 1982. Volcaniclastic rocks of the Reydarfjordur Drill Hole, eastern Iceland. 2: Alteration. *J. Geophys. Res.*, 87:6459–6476.
- Viereck, L. G., Simon, M., Schmincke, H.-U., 1986. Primary composition, alteration and origin of Cretaceous volcaniclastic rocks, East Mariana Basin (Site 585, Leg 89). In Moberly, R., Schlanger, S. O., et al., *Init. Repts. DSDP*, 89: Washington (U.S. Govt. Printing Office), 529–553.
- Wilkinson, J.F.G., 1956. Clinopyroxenes of alkali basalt magma. *Am. Mineral.*, 41:724–743.
- Winterer, E. L., 1973. Regional problems. In Winterer, E. L., Ewing, J. I., et al., *Init. Repts. DSDP*, 17: Washington (U.S. Govt. Printing Office), 911–922.
- Zhou, Z., and Fyfe, W. S., 1989. Palagonitization of basaltic glass from DSDP Site 335, Leg 37: textures, chemical composition and mechanism of formation. *Am. Mineral.*, 74:1045–1053.

Date of initial receipt: 3 June 1991

Date of acceptance: 20 February 1992

Ms 129B-114

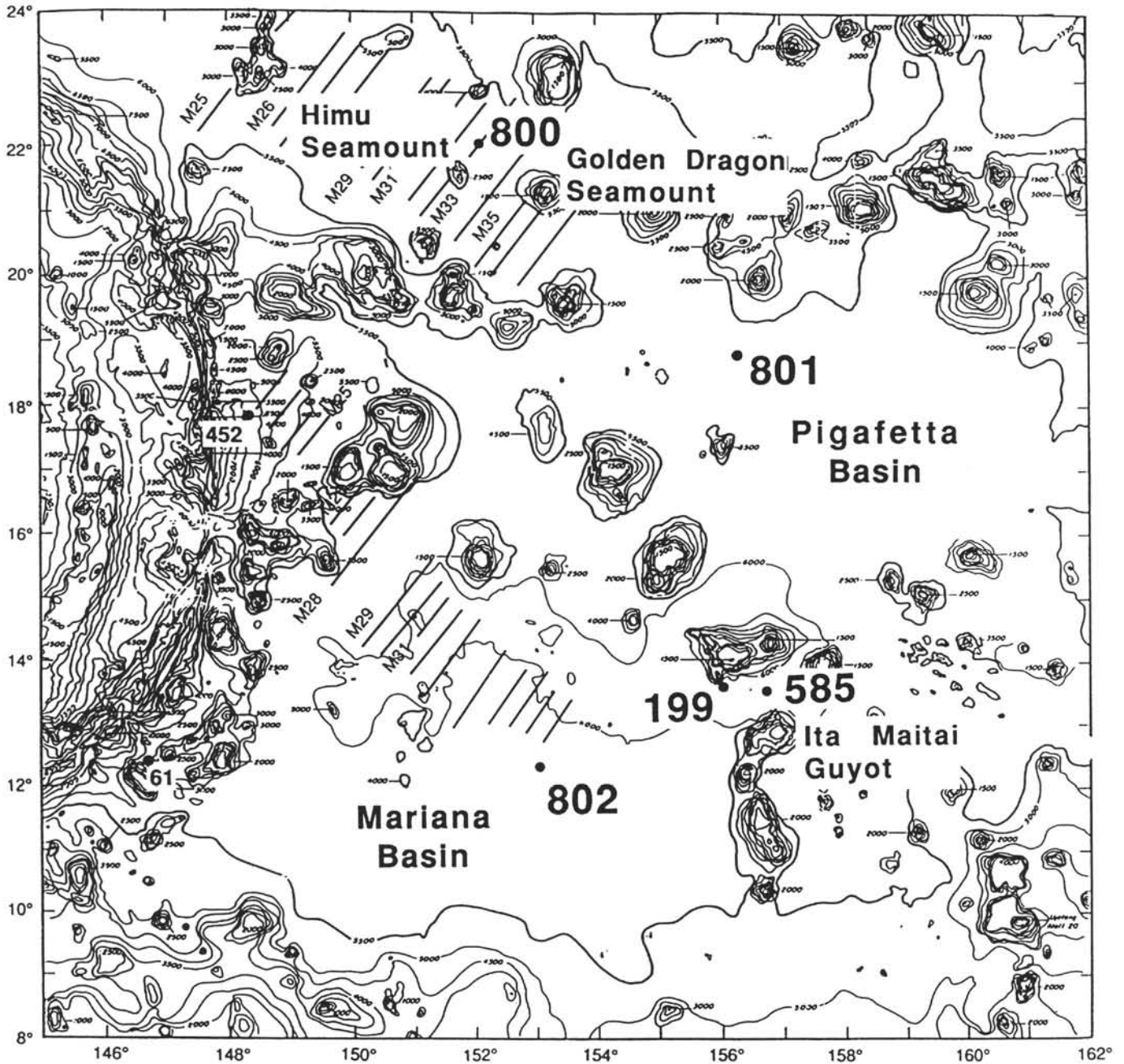


Figure 12. Bathymetry (in meters) of the central western Pacific Ocean (Lancelot, Larson, et al., 1990), showing location of Sites 800, 801, and 802. Sources for the Cretaceous volcanoclastites are probably represented by seamounts surrounding the different sites, although the Miocene materials at Site 802 were derived from the Eastern Caroline Islands submarine platform well to the south. Magnetic anomalies and DSDP sites also shown for reference.

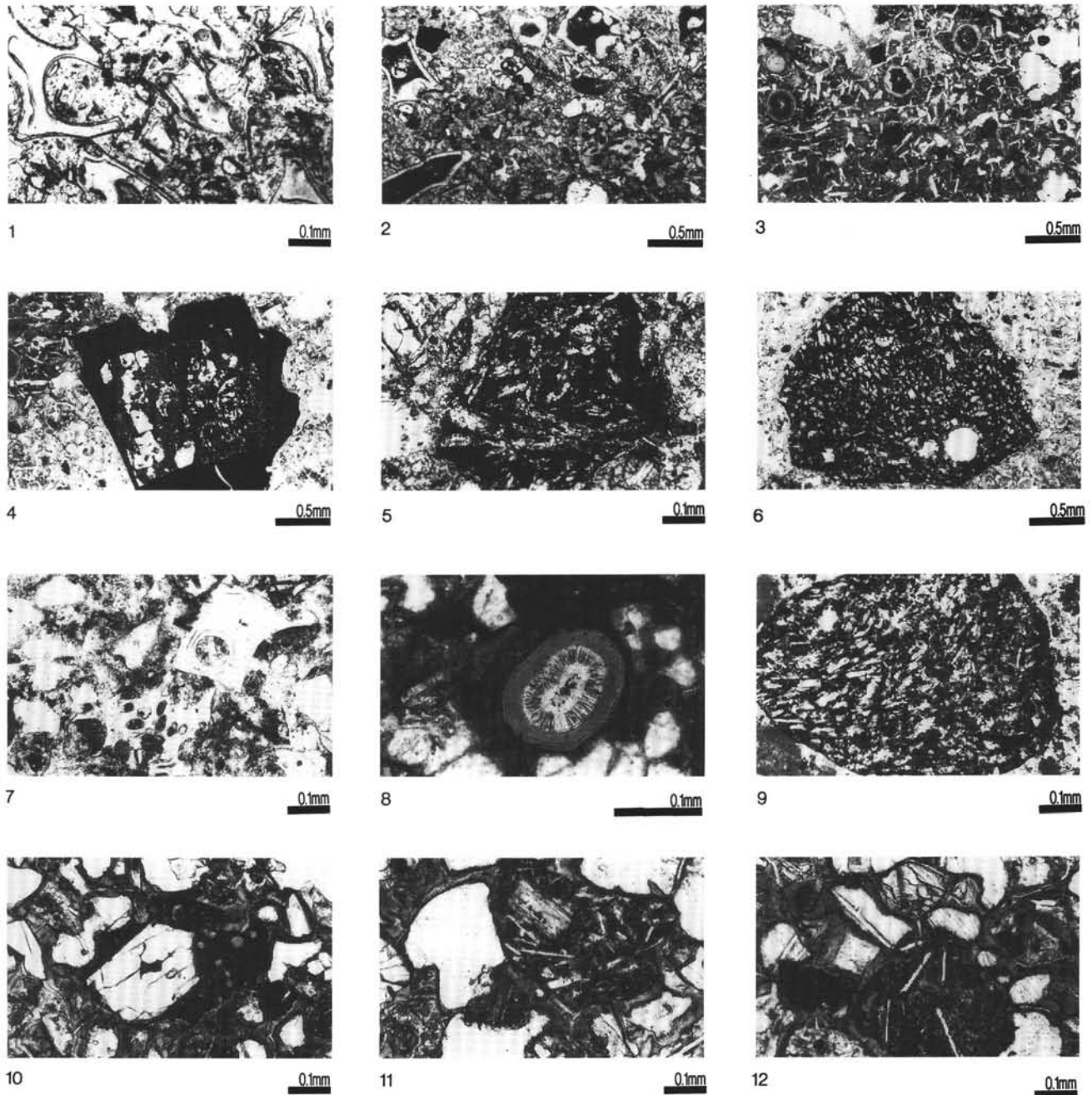


Plate 1. Textural and petrographic features of Miocene (1–6) and Cretaceous (7–12) volcaniclastic sediments from Leg 129. All photomicrographs taken in plane polarized light. **1.** Cusped, pale yellow sideromelane shards, with shapes governed by vesicle walls, in a smectitic matrix. Sample 129-802A-8R-1, 106–107 cm. **2.** Broken palagonite shards with dark, smectite-replaced interiors set in a mixed microshard-smectite matrix. Sample 129-802A-4R-1, 95–97 cm. **3.** Vesicular palagonite shard with small, irregular shrinkage cracks, microphenocrysts of plagioclase, and larger, partly released clinopyroxene phenocrysts. Sample 129-802A-15R-1, 133–135 cm. **4.** Dark, angular tachylite clast with partly altered clinopyroxene megaphenocryst. Sample 129-802A-15R-1, 133–135. **5.** Dark, tachylite clast with plumose quench crystals of clinopyroxene. Sample 129-802A-6R-2, 60–62 cm. **6.** Oxidized, dark, hypocrySTALLINE basalt clast with granular clinopyroxene and plagioclase microlites. Sample 129-802A-15R-1, 133–135 cm. **7.** Vesicular, pale yellow palagonite shards in fine-grained smectitic matrix. Sample 129-801B-1R-3, 17–18 cm. **8.** Amygdale in tachylite clast with concentric zones of greenish fibrous smectites. Sample 129-800A-33R-5, 127–130 cm. **9.** HypocrySTALLINE basalt clast with flow-aligned plagioclase microlites. Sample 129-800A-32R-1, 117–118 cm. **10.** Vesicular, dark tachylite clast with clinopyroxene megaphenocryst. Sample 129-800A-26R-3, 56–58 cm. **11.** Dark, holocrySTALLINE basalt clast with opaque ore, plagioclase microlites, and microphenocryst of clinopyroxene. Sample 129-800A-26R-3, 56–58 cm. **12.** Admixture of dark tachylite, hypocrySTALLINE basalt, phyrlic (altered) glass, and cracked pyroxene clasts in carbonate-smectite matrix. Sample 129-800A-26R-3, 56–58 cm.